Optimal orbit transfer of single-tether E-sail with inertially fixed spin axis

Alessandro A. Quarta (✉), **Marco Bassetto, and Giovanni Mengali**

Department of Civil and Industrial Engineering, University of Pisa, Pisa I-56122, Italy

ABSTRACT

This study analyzes the optimal transfer trajectory of a spacecraft propelled by a spin-stabilized electric solar wind sail (E-sail) with a single conducting tether and a spin axis with a fixed direction in an inertial (heliocentric) reference frame. The approach proposed in this study is useful for rapidly analyzing the optimal transfer trajectories of the current generation of small spacecraft designed to obtain *in-situ* evidence of the E-sail propulsion concept. In this context, starting with the recently proposed thrust model for a single-tether E-sail, this study discusses the optimal control law and performance in a typical two-dimensional interplanetary transfer by considering the (binary) state of the onboard electron emitter as the single control parameter. The resulting spacecraft heliocentric trajectory is a succession of Keplerian arcs alternated with propelled arcs, that is, the phases in which the electron emitter is switched on. In particular, numerical simulations demonstrated that a single-tether E-sail with an inertially fixed spin axis can perform a classical mission scenario as a circle-to-circle two-dimensional transfer by suitably varying a single control parameter.

KEYWORDS

electric solar wind sail (E-sail)
single conducting tether
fixed inertial spin axis
trajectory optimization
circle-to-circle coplanar transfer

Research Article

Received: 17 September 2023
Accepted: 15 December 2023

1 Introduction

This paper analyzes the optimal performance of an interplanetary spacecraft propelled by an electric solar wind sail (E-sail) [1, 2] with an unconventional configuration comprising a single conducting tether that spins around a fixed inertial direction. In fact, the usual E-sail arrangement comprises various conductive tethers connected to the spacecraft main body [3, 4], which are deployed and maintained stretched by spinning the vehicle around its symmetry axis [5]. Although such a configuration allows the designer to fine-tune the propulsive performance by selecting both the number of cables and tether length [6], it requires a rather complex spacecraft design in terms of tether reeling [7, 8] and deployment mechanisms [9].

Therefore, as described in the recent review paper by the authors [10], the in-space validation of the E-sail propulsion concept will be left to a small spacecraft (probably a CubeSat [11–13]) with a single conducting tether of some hundred meters in length [14–16]; see the conceptual scheme of Fig. 1, which describes the proposed ESTCube Lunar Cubesat E-Sail Experiment [17].

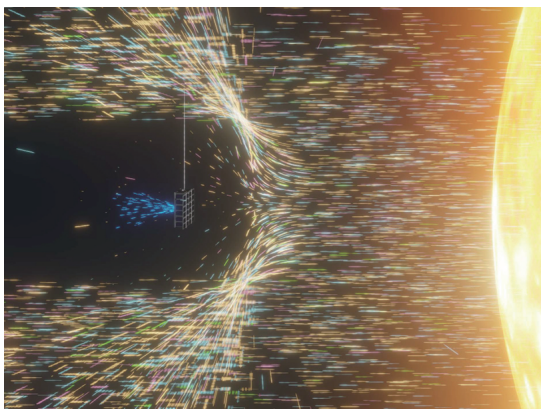

Fig. 1 Artistic impression of CubeSat with a spinning, single-tether, E-sail. Image courtesy of Mario F. Palos.

Because the thrust vector of such a configuration cannot be described by the geometric formulation

✉ a.quarta@ing.unipi.it

Nomenclature

$\boldsymbol{a}$	propulsive acceleration vector (mm/s^2)
a_c	characteristic acceleration (mm/s^2)
C	spacecraft center of mass
$\hat{\boldsymbol{d}}$	auxiliary unit vector
$\boldsymbol{e}$	error vector
E	endpoint Lagrangian
$\boldsymbol{f}$	dynamics vector
h	orbital angular momentum magnitude (km^2/s)
H	Hamiltonian function
$\mathcal{H}$	maximized Hamiltonian
H_c	part of H that depends on the control
$\{\hat{\boldsymbol{i}}, \hat{\boldsymbol{j}}, \hat{\boldsymbol{k}}\}$	unit vectors of $\mathcal{T}$
J	cost function
O	Sun's center of mass
r	orbital radius (au)
$\hat{\boldsymbol{r}}$	radial unit vector
t	time (years)
$\hat{\boldsymbol{t}}$	transverse unit vector
$\mathcal{T}$	body reference frame
$\mathcal{T}_\odot$	heliocentric reference frame
u	radial component of spacecraft velocity (km/s)
$\boldsymbol{x}$	spacecraft state vector
$\{x, y, z\}$	axes of $\mathcal{T}$
α_d	angle between $\hat{\boldsymbol{d}}$ and $\hat{\boldsymbol{r}}$ (rad)
α_λ	primer vector angle (rad)
α_0	auxiliary angle (rad)
β	dimensionless form of a_c
θ	polar angle (rad)
$\boldsymbol{\lambda}$	costate vector
$\boldsymbol{\lambda}_\mathrm{p}$	primer vector with $\lambda_\mathrm{p} = \Vert\boldsymbol{\lambda}_\mathrm{p}\Vert$
$\{\lambda_\mathrm{r}, \lambda_\theta, \lambda_u, \lambda_h\}$	costates
$\mu_\odot$	Sun's gravitational parameter (km^3/s^2)
τ	dimensionless control parameter
ω	spacecraft spin rate (rad/s)
Subscripts	
f	final
0	initial, at time $t_0 \triangleq 0$
$\oplus$	at 1 au from the Sun
Superscripts	
$\dot{}$	time derivative
$\bar{}$	mean value
$\wedge$	unit vector
$\star$	optimal

discussed by Huo *et al.* [18], which is valid for a multi-tether E-sail, the authors recently proposed a specific mathematical model [19] to estimate the propulsive acceleration of a low-performance E-sail with a single conducting tether. In particular, the model proposed in Ref. [19], which is briefly summarized in Section 2, shows that the average propulsive acceleration of a single-tether arrangement can be reduced to a single-vectorial equation. Moreover, Ref. [19] also indicated how this single-tether thrust model can be used to describe the two-dimensional dynamics of an E-sail-based spinning spacecraft with a fixed inertial direction of the spin axis. This is a rather important scenario because it models the typical behavior of a spinning single-tether CubeSat with reduced control authority [17], in which the spin plane is substantially fixed with respect to an inertial frame. In this case, the spacecraft has a single binary control parameter, that is, the state of the onboard electron emitter, which determines the state of charge of the single tether. In this context, the natural question is whether a single-tether E-sail with a fixed attitude can be used in classical heliocentric orbit transfers.

The main contribution of this study is to answer this important question. Using the authors' recent thrust model [19], this paper discusses the control law and minimum time trajectories in a typical heliocentric mission scenario. More precisely, a circle-to-circle two-dimensional orbit transfer was parametrically studied in an optimal framework using an indirect method, assuming a fixed sail inertial attitude and a single control variable related to the (binary) power state of the onboard electron emitter. Numerical simulations show that, in this highly constrained mission scenario, a suitable control law allows the spacecraft to complete a circular orbit raising (or lowering) with flight time depending on the maximum magnitude of the E-sail propulsive acceleration at a reference distance.

2 Mathematical preliminaries

This section summarizes the main analytical results obtained in recent literature [19] in the context of a single-tether E-sail with a fixed inertial attitude. This mathematical foundation is the starting point for the trajectory optimization process illustrated in Section 3, which constitutes one of the contributions of this study.

Consider a spacecraft propelled by a single-tether E-sail that rotates at a constant spin rate ω around the z-axis of a right-handed reference frame $\mathcal{T}(C; x, y, z)$ with unit vectors $\{\hat{\boldsymbol{i}}, \hat{\boldsymbol{j}}, \hat{\boldsymbol{k}}\}$. The origin C of $\mathcal{T}$ coincides

with the center of mass of the spacecraft and the x-axis is aligned with the conducting tether. Plane $(\hat{\boldsymbol{i}}, \hat{\boldsymbol{j}})$, which is perpendicular to the spin-unit vector $\hat{\boldsymbol{k}}$, coincides with the E-sail nominal plane [20]; see Fig. 2.

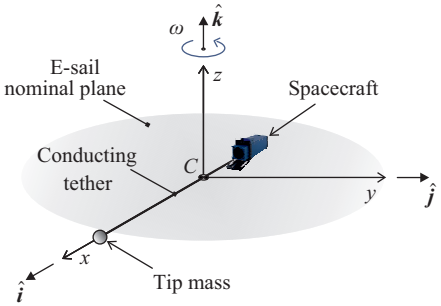

Fig. 2 Conceptual scheme of an E-sail-based spacecraft with a single, spinning, conducting tether. Reproduced with permission from Ref. [19], © Elsevier Masson SAS 2023.

According to Ref. [19], the propulsive acceleration vector $\boldsymbol{a}$ given by a single-tether E-sail can be analytically described as Eq. (1):

$$\boldsymbol{a} = \frac{a_{\mathrm{c}}\tau}{2}\left(\frac{r_{\oplus}}{r}\right)\left[\hat{\boldsymbol{r}} - \left(\hat{\boldsymbol{r}}\cdot\hat{\boldsymbol{i}}\right)\hat{\boldsymbol{i}}\right] \tag{1}$$

where r is the Sun–spacecraft distance, $r_{\oplus} = 1$ au is a reference distance, $\hat{\boldsymbol{r}}$ is the Sun–spacecraft (or radial) unit vector, $\tau \in \{0; 1\}$ is a dimensionless term that models the on/off mode of the onboard electron emitter, and a_{c} is the characteristic acceleration, which is the typical performance parameter of an E-sail-based spacecraft [21] and coincides with the maximum value of $\|\boldsymbol{a}\|$ when $r = r_{\oplus}$. Note that $\boldsymbol{a}$ depends on the azimuthal position of the conducting tether on the E-sail nominal plane (i.e., in the time-varying direction of $\hat{\boldsymbol{i}}$) such that the components of the propulsive acceleration vector change during the rotation of the spacecraft around its spin axis. To avoid this problem and obtain a simple expression suitable for a preliminary trajectory design at a generic time instant t, the thrust model in Ref. [19] uses a mean acceleration value $\overline{\boldsymbol{a}}$ computed over one spin period centered at t, which is given by

$$\overline{\boldsymbol{a}} \triangleq \frac{\omega}{2\pi}\int_{t-\pi/\omega}^{t+\pi/\omega} \boldsymbol{a}\mathrm{d}t \approx \frac{a_{\mathrm{c}}\tau}{2}\left(\frac{r_{\oplus}}{r}\right)\left[\hat{\boldsymbol{r}} + \left(\hat{\boldsymbol{r}}\cdot\hat{\boldsymbol{k}}\right)\hat{\boldsymbol{k}}\right] \tag{2}$$

The expression of $\overline{\boldsymbol{a}}$, which may be considered as a special case of the multi-tether thrust model discussed in Ref. [18], is useful for describing the spacecraft dynamics in a heliocentric mission scenario, where the flight time is several orders of magnitude higher than the spacecraft spin period [22]. Now, we investigate a two-dimensional transfer problem with the following two assumptions: (i) the spin axis z is along the plane of the spacecraft osculating orbit at the initial time $t_0 = 0$ and (ii) the direction of $\hat{\boldsymbol{k}}$ is fixed with respect to an inertial reference frame. Notably, changing the E-sail inertial attitude (or varying the inertial orientation of the sail nominal plane) is a complex task for a single-tether configuration [22, 23]. Therefore, a possible simplification of the E-sail guidance law is to maintain a fixed inertial direction of the spacecraft's spin axis, which amounts to assuming $\hat{\boldsymbol{k}} \equiv \hat{\boldsymbol{k}}_0 \triangleq \hat{\boldsymbol{k}}(t_0)$ for $t \geqslant t_0$. In particular, the direction of $\hat{\boldsymbol{k}}_0$ is determined by the auxiliary angle $\alpha_0 \in [-\pi/2, \pi/2]$ rad, which is defined as the angle between the direction of $\hat{\boldsymbol{k}}_0$ and the Sun–spacecraft line at the initial time t_0; see Fig. 3, where r_0 denotes the initial radial distance.

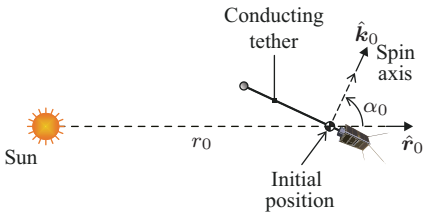

Fig. 3 Spacecraft initial position and auxiliary angle α_0.

In this case, the average acceleration $\overline{\boldsymbol{a}}$ is conveniently written in a polar reference frame $\mathcal{T}_{\odot}(O; r, \theta)$ with unit vectors $(\hat{\boldsymbol{r}}, \hat{\boldsymbol{t}})$, the origin of which coincides with the Sun's center of mass, θ is the polar angle measured counterclockwise from the Sun–spacecraft line at time t_0, and $\hat{\boldsymbol{t}} \triangleq \hat{\boldsymbol{h}} \times \hat{\boldsymbol{r}}$ is the transverse unit vector, where $\hat{\boldsymbol{h}}$ is the unit vector of the orbital angular momentum. From Eq. (2), we obtain

$$\overline{\boldsymbol{a}} = a_{\mathrm{r}}\hat{\boldsymbol{r}} + a_{\mathrm{t}}\hat{\boldsymbol{t}} \tag{3}$$

where a_{r} and a_{t} are the radial and transverse components of propulsive acceleration, respectively. In particular, a_{r} and a_{t} are given by

$$a_{\mathrm{r}} = \frac{\beta\tau}{2}\frac{\mu_{\odot}}{r r_{\oplus}}\left(1 + \cos^2(\alpha_0 - \theta)\right) \tag{4}$$

$$a_{\mathrm{t}} = \frac{\beta\tau}{2}\frac{\mu_{\odot}}{r r_{\oplus}}\sin(\alpha_0 - \theta)\cos(\alpha_0 - \theta) \tag{5}$$

where $\mu_{\odot}$ is the gravitational parameter of the Sun and β is a dimensionless form of a_{c}, defined as

$$\beta = \frac{a_{\mathrm{c}}}{\mu_{\odot}/r_{\oplus}^2} \tag{6}$$

where $\mu_{\odot}/r_{\oplus}^2 \approx 5.93$ mm/s^2. The dimensionless (binary) term τ is the only control parameter in Eqs. (4) and

(5). Accordingly, the heliocentric trajectory of a single-tether E-sail with a fixed inertial attitude is a succession of Keplerian arcs (when $\tau = 0$) that alternates with propelled arcs (when $\tau = 1$).

Bearing in mind Eqs. (3)–(5), the heliocentric spacecraft dynamics is described by the nonlinear equations of motion:

$$\dot{\boldsymbol{x}}(t) = \boldsymbol{f}(\boldsymbol{x}(t), \tau(t)) \tag{7}$$

with

$$\boldsymbol{f} \triangleq \begin{bmatrix} u \\ h/r^2 \\ -\mu_\odot/r^2 + h^2/r^3 + a_\mathrm{r} \\ r a_\mathrm{t} \end{bmatrix}$$

where u is the radial component of the spacecraft's inertial velocity, h is the magnitude of the angular momentum vector, and $\boldsymbol{x}$ is the spacecraft state vector, defined as Eq. (8):

$$\boldsymbol{x} \triangleq [r,\ \theta,\ u,\ h]^\mathrm{T} \tag{8}$$

whose initial value is

$$\boldsymbol{x}(t_0) = \boldsymbol{x}_0 \triangleq [r_0,\ \theta_0,\ u_0,\ h_0]^\mathrm{T} \tag{9}$$

The single-tether thrust model and previous equations of motion are used in Section 3 to analyze the optimal transfer trajectory in a classical heliocentric mission scenario.

3 Optimal control law and trajectory analysis

The optimal spacecraft trajectory is obtained using an indirect approach [24, 25] based on Pontryagin's maximum principle [26–28]. In this respect, to obtain a result that can also be used in a locally-optimal control law [29], the first step is to determine the value $\tau^\star$ that maximizes the projection of $\overline{\boldsymbol{a}}$ along a (prescribed) generic direction [30]. The latter is described by the unit vector:

$$\hat{\boldsymbol{d}} \triangleq \cos\alpha_d \hat{\boldsymbol{r}} + \sin\alpha_d \hat{\boldsymbol{t}} \tag{10}$$

where $\alpha_d \in [-\pi, \pi]$ rad is an auxiliary angle defined as the angle between $\hat{\boldsymbol{d}}$ and $\hat{\boldsymbol{r}}$ (see the scheme in Fig. 4). Note that $\alpha_d \geqslant 0$ when $\hat{\boldsymbol{d}} \cdot \hat{\boldsymbol{t}} \geqslant 0$ and $\alpha_d < 0$ when $\hat{\boldsymbol{d}} \cdot \hat{\boldsymbol{t}} < 0$.

The problem of maximizing the projection of $\overline{\boldsymbol{a}}$ along $\hat{\boldsymbol{d}}$ involves maximizing the projection of $\overline{\boldsymbol{a}}$ along $\hat{\boldsymbol{d}}$. To that end, bearing in mind Eqs. (4) and (5), consider the cost function J defined as

$$J \triangleq \overline{\boldsymbol{a}} \cdot \hat{\boldsymbol{d}} = \frac{\beta}{2} \frac{\mu_\odot}{r r_\oplus} \tau [(1 + \cos^2(\alpha_0 - \theta)) \cos\alpha_d + \sin(\alpha_0 - \theta) \cos(\alpha_0 - \theta) \sin\alpha_d] \tag{11}$$

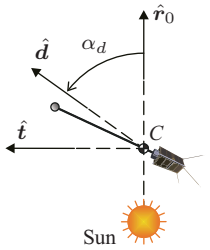

Fig. 4 Sketch of the unit vector $\hat{\boldsymbol{d}}$ and the auxiliary angle α_d.

For a given triplet $\{\theta, \alpha_0, \alpha_d\}$, the value of τ that maximizes J is

$$\tau = \tau^\star \triangleq \frac{\mathrm{sign}((1 + \cos^2(\alpha_0 - \theta)) \cos\alpha_d + \sin(\alpha_0 - \theta) \cos(\alpha_0 - \theta) \sin\alpha_d) + 1}{2} \tag{12}$$

where sign(□) denotes the signum function.

The general results for Eq. (12) can be used to obtain the optimal control law using variational calculus. Although the procedure described below can be easily extended to more complex mission cases, we limit our discussion to the classical circle-to-circle orbit transfer, in which the spacecraft initially traces a circular heliocentric orbit of a given radius r_0. The initial state vector $\boldsymbol{x}_0$ defined in Eq. (9) becomes

$$\boldsymbol{x}_0 \triangleq [r_0, 0, 0, \sqrt{\mu_\odot r_0}]^\mathrm{T} \tag{13}$$

where the initial polar angle θ_0 is set to zero without loss of generality. As is typical in E-sail mission design [5, 10], the transfer trajectory is obtained by minimizing the flight time t_f necessary for the spacecraft to be placed in a circular coplanar orbit of a given radius $r_\mathrm{f} \neq r_0$. The optimization problem consists of finding the optimal control law $\tau(t)$ that maximizes the performance index $\mathcal{J} \triangleq -t_\mathrm{f}$ subject to the nonlinear dynamics (7), the initial constraints (13), and the final constraint:

$$\boldsymbol{e}(t_\mathrm{f}) = \boldsymbol{0} \tag{14}$$

with

$$\boldsymbol{e}(t_\mathrm{f}) \triangleq \begin{bmatrix} r(t_\mathrm{f})/r_\mathrm{f} - 1 \\ u(t_\mathrm{f})/\sqrt{\mu_\odot/r_0} \\ h(t_\mathrm{f})/\sqrt{\mu_\odot r_0} - \sqrt{r_\mathrm{f}/r_0} \end{bmatrix}$$

where the final polar angle $\theta(t_\mathrm{f})$ is left free.

By paralleling the general procedure described in Ref. [26], given an optimal solution, there exists an absolutely continuous covector function $\boldsymbol{\lambda}$ and covector $\boldsymbol{\nu}$ that satisfy the adjoint equations, the Hamiltonian maximization condition, the Hamiltonian value condition, the Hamiltonian evolution equation,

and the transversality condition. In particular, the Hamiltonian function H and the Endpoint Lagrangian E are given by

$$H = \boldsymbol{\lambda}^{\mathrm{T}} \boldsymbol{f}(\boldsymbol{x}(t), \tau(t)),\ E = -t_{\mathrm{f}} + \boldsymbol{\nu}^{\mathrm{T}} \boldsymbol{e}(t_{\mathrm{f}}) \tag{15}$$

where the covector

$$\boldsymbol{\lambda} \triangleq [\lambda_{\mathrm{r}}, \lambda_\theta, \lambda_u, \lambda_h]^{\mathrm{T}} \tag{16}$$

is the vector of the adjoint variables $\{\lambda_{\mathrm{r}}, \lambda_\theta, \lambda_u, \lambda_h\}$ associated with the spacecraft states $\{r, \theta, u, h\}$. The adjoint equations are as Eq. (17):

$$\dot{\boldsymbol{\lambda}} = -\frac{\partial H}{\partial \boldsymbol{x}} \tag{17}$$

According to Pontryagin's maximum principle, the Hamiltonian maximization condition amounts to maximizing, at any time, the Hamiltonian function with respect to the control variable τ. Therefore, the maximized Hamiltonian:

$$\mathcal{H} \triangleq \max_{\tau}(H) \tag{18}$$

is obtained by maximizing the portion of H (namely, H_{c}) that explicitly depends on the control, that is

$$H_{\mathrm{c}} \triangleq \lambda_u a_{\mathrm{r}} + \lambda_h r a_{\mathrm{t}} \tag{19}$$

By substituting Eqs. (4) and (5) into Eq. (19), the latter becomes

$$\begin{aligned} H_{\mathrm{c}} = \lambda_{\mathrm{p}} \frac{\beta\tau}{2} \frac{\mu_\odot}{r r_\oplus} [(1 + \cos^2(\alpha_0 - \theta)) \cos\alpha_\lambda \\ + \sin(\alpha_0 - \theta) \cos(\alpha_0 - \theta) \sin\alpha_\lambda] \end{aligned} \tag{20}$$

where $\lambda_{\mathrm{p}} \triangleq \sqrt{\lambda_u^2 + r^2\lambda_h^2}$ is the magnitude of Lawden's primer vector $\boldsymbol{\lambda}_{\mathrm{p}} \triangleq [\lambda_u, r, \lambda_h]^{\mathrm{T}}$ [30] and the auxiliary angle $\alpha_\lambda \in [0, 2\pi)$ rad is implicitly defined from

$$\lambda_u = \lambda_{\mathrm{p}} \cos\alpha_\lambda,\ r\lambda_h = \lambda_{\mathrm{p}} \sin\alpha_\lambda \tag{21}$$

A comparison of Eqs. (11) and (20) indicates that the optimal control law is equivalent to Eq. (12) by simply substituting α_d with α_λ, that is

$$\tau = \frac{\begin{array}{c}\mathrm{sign}((1 + \cos^2(\alpha_0 - \theta))(\lambda_u/\lambda_{\mathrm{p}}) \\ + \sin(\alpha_0 - \theta)\cos(\alpha_0 - \theta)(\lambda_h/\lambda_{\mathrm{p}}))\end{array} + 1}{2} \tag{22}$$

The Hamiltonian value condition [26] provides the value of $\mathcal{H}$ at final time t_{f}, which is given by

$$\mathcal{H}(\boldsymbol{\lambda}(t_{\mathrm{f}}), \boldsymbol{x}(t_{\mathrm{f}})) = -\frac{\partial E}{\partial t_{\mathrm{f}}} = 1 \tag{23}$$

while the Hamiltonian evolution equation states that

$$\frac{\mathrm{d}\mathcal{H}}{\mathrm{d}t} = \frac{\partial H}{\partial t} = 0 \tag{24}$$

where the last equality follows from the fact that the dynamic system (7) is autonomous, so that the maximized Hamiltonian is a constant of motion. In particular, by considering Eq. (23), we obtain

$$\mathcal{H}(t) \equiv \mathcal{H}(t_{\mathrm{f}}) = 1 \tag{25}$$

Finally, the optimal solution satisfies the transversality conditions:

$$\boldsymbol{\lambda}(t_{\mathrm{f}}) = \frac{\partial E}{\partial \boldsymbol{x}(t_{\mathrm{f}})} \tag{26}$$

from which

$$\lambda_\theta(t_{\mathrm{f}}) = 0 \tag{27}$$

Therefore, the two-point boundary value problem associated with the optimization procedure requires the calculation of the flight time t_{f} and the initial value of the adjoint variables $\{\lambda_{\mathrm{r}}, \lambda_\theta, \lambda_u, \lambda_h\}$ by enforcing the final constraints given by Eqs. (14), (25), and (27), respectively.

4 Model validation and numerical simulations

In this section, we present a set of numerical simulations for the previously discussed optimal control law. In particular, the proposed solution was first compared with the approximate analytical solution obtained in Ref. [19], where a locally optimal control law that maximizes the local value of the θ-variation of the angular momentum magnitude was used to obtain a (nearly) circle-to-circle orbit transfer. Specifically, Ref. [19] described an approximate method to estimate the required characteristic acceleration as a function of the initial and final orbit radii and the number n of complete revolutions during the transfer. The approximate model in Ref. [19] requires a low-performance E-sail, while the approach of this study is more general as is valid for any value of characteristic acceleration.

Second, we analyzed heliocentric transfers that model classical ephemeris-free mission scenarios from the Earth to Mars or Venus. In all numerical simulations, a value of $r_0 = r_\oplus$ was assumed, which is consistent with a spacecraft that leaves the Earth's sphere of influence on a parabolic escape trajectory, with the simplifying assumption that the Earth's heliocentric orbit is circular and coplanar to the target circular orbit.

4.1 Comparison with approximate literature results

According to the approximate analytical solution illustrated in Ref. [19], when $r_{\mathrm{f}} \in \{1.1, 0.9\}$ au and

the number of complete revolutions around the Sun is $n = 5$, we obtain $\beta \approx \{0.0182, 0.0222\}$, which corresponds to $a_c \approx \{0.1078, 0.1318\}$ mm/s^2. Using the approach proposed in the previous section and assuming the same values of r_f and β (or a_c), we obtain the optimal transfer trajectories shown in Fig. 5. As expected, the figure indicates that the transfer obtained through the (exact) optimal approach in this study is better than that obtained with the approximate method. Note, in fact, that the orbit transfer is completed in (slightly) less than five revolutions around the Sun.

Figure 6 shows the time evolutions of the states in the two cases, where $v \triangleq h/r$ represents the transverse component of the spacecraft velocity. The gray bars correspond to the time intervals with $\tau = 1$, that is, the time intervals in which the E-sail provides a propulsive acceleration. The number of revolutions is similar to that estimated by the analytical approximation. Finally, Fig. 7 shows a comparison between the optimal and approximate variations in h/h_0 and θ for the two compared cases. It can be seen that the analytical solution given by Ref. [19], which is valid for a medium–low-performance E-sail, approximates well the optimal solution.

4.2 Potential mission scenarios

The proposed mathematical model is now used to analyze two classical, circle-to-circle, interplanetary transfers with a medium–high-performance E-sail. In particular, the radius of the target orbit is either $r_f = 1.524$ au or $r_f = 0.723$ au, which correspond to the simplified ephemeris-free Earth–Mars and Earth–Venus transfer, respectively. In this context, Fig. 8 shows the variations in the minimum flight time t_f and final polar angle $\theta(t_f)$ with a characteristic acceleration in the range $a_c \in [0.2, 1]$ mm/s^2 when $\alpha_0 = 0$, whereas Fig. 9 shows the variations in t_f and $\theta(t_f)$ with $\alpha_0 \in [-90, 90]$ deg when $a_c = 0.2$ mm/s^2 (or $\beta \approx 0.0337$). Finally, Fig. 10 shows the optimal transfer trajectories (black line) for the two mission scenarios as a function of a_c when $\alpha_0 = 0$. In this figure, the blue (or red) line indicates the Earth's (or the target planet) orbit.

The numerical results indicate that the two-dimensional circle-to-circle orbit raising (or lowering) of practical interest can be obtained by spinning a single-tether E-sail with an inertially fixed spin axis using a suitable control law involving a single control parameter, that is, the on/off state of the electron emitter. In this case, the transfer performance is strongly related to the value of the sail characteristic acceleration, whereas the dependence of the flight time on α_0 is less pronounced. In the two interplanetary mission scenarios considered in this section, the numerical simulations also show that the flight time of an E-sail with an inertially fixed spin axis is significantly greater than that obtained with the corresponding E-sail of variable attitude, that is, an E-sail with two control parameters (i.e., electron emitter state and sail pitch angle).

For example, when $\alpha_0 = 0$, an E-sail with a characteristic acceleration of 0.5 mm/s^2 completes an Earth–Mars (or an Earth–Venus) transfer of approximately 5.7 years (or 3.5 years) with approximately four revolutions around the Sun. However, an E-sail with

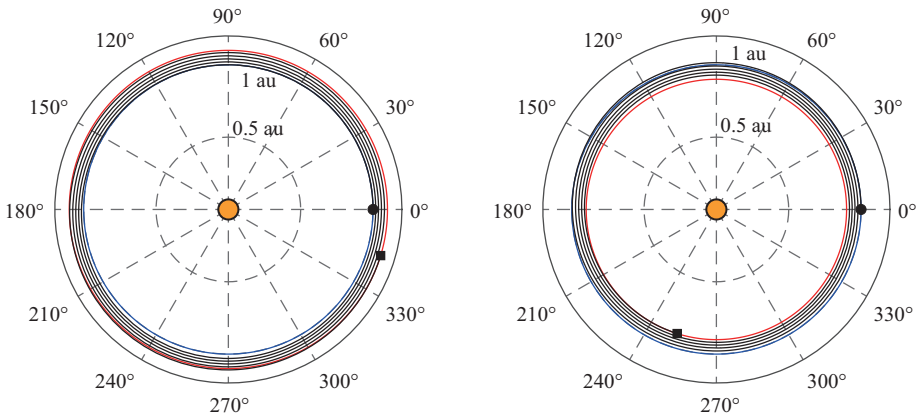

(a) $r_f = 1.1$ au and $\beta \approx 0.0182$ (b) $r_f = 0.9$ au and $\beta \approx 0.0222$

Fig. 5 Optimal transfer trajectory (black line), when $r_0 = 1$ au, for two mission scenarios. Blue line → parking orbit; red line → target orbit; black circle → start; black square → arrival; orange circle → the Sun.

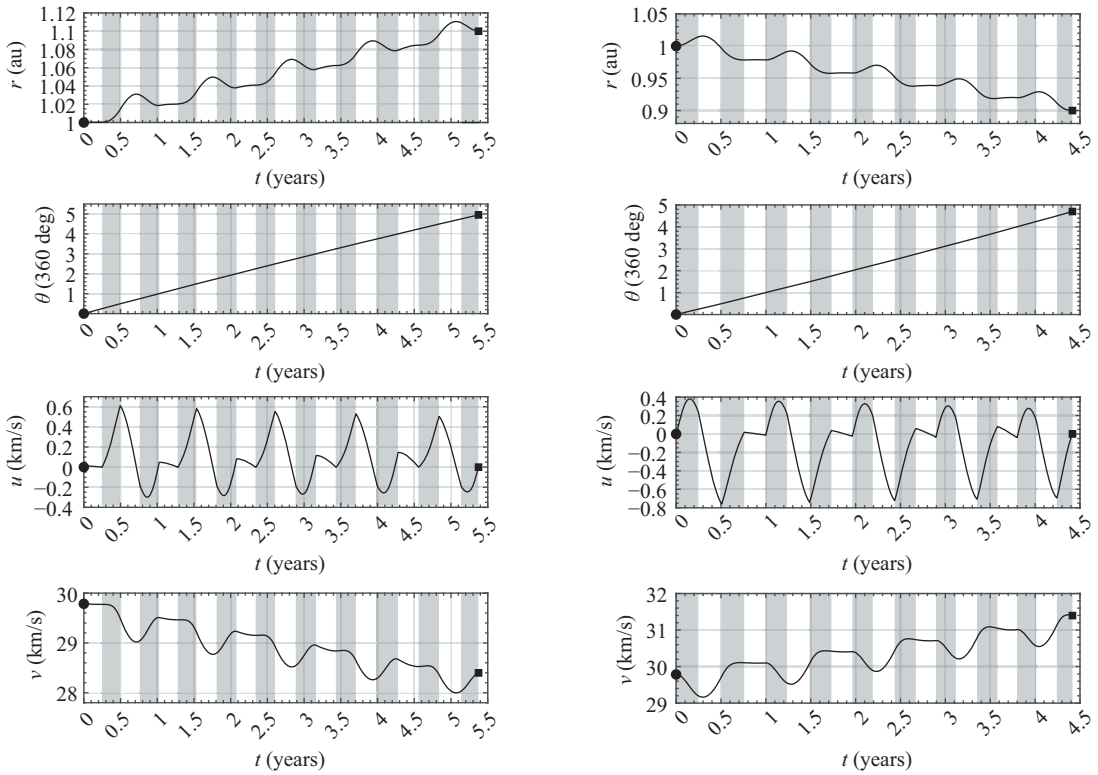

(a) $r_f = 1.1$ au and $\beta \approx 0.0182$ (b) $r_f = 0.9$ au and $\beta \approx 0.0222$

Fig. 6 Time-evolutions of the state variables when $r_0 = 1$ au, for two mission scenarios.

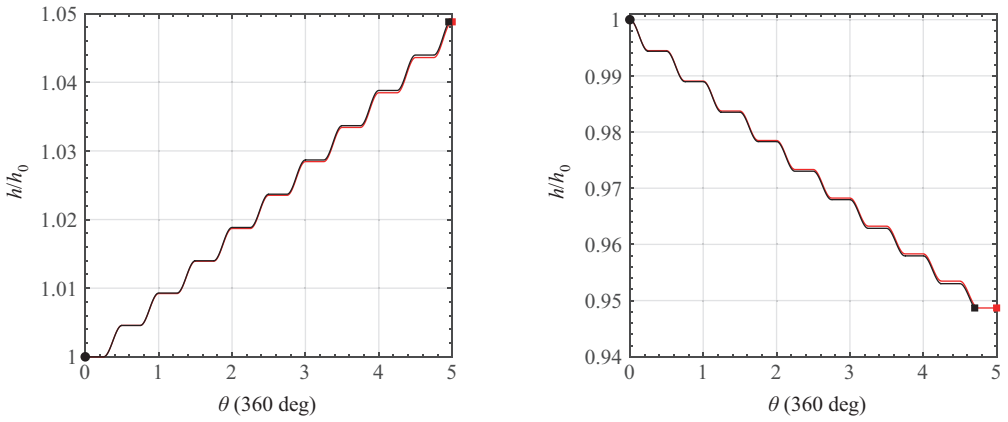

(a) $r_f = 1.1$ au and $\beta \approx 0.0182$ (b) $r_f = 0.9$ au and $\beta \approx 0.0222$

Fig. 7 Comparison between optimal (black lines) and approximate (red lines) variations of h/h_0 obtained through the method described in Ref. [19].

the same characteristic acceleration completes the Earth–Mars (or an Earth–Venus) transfer in approximately 2 years (or 1.4 years) in less than two revolutions around the Sun if it can change both the pitch angle and the electron emitter state. A performance comparison in terms of minimum flight time as a function of a_c between an E-sail with an inertially fixed spin axis and an E-sail with two control parameters is summarized in Table 1.

The table shows that, in some cases, the flight time required by an E-sail with a single control parameter is approximately three times greater than that required by an E-sail with two control parameters.

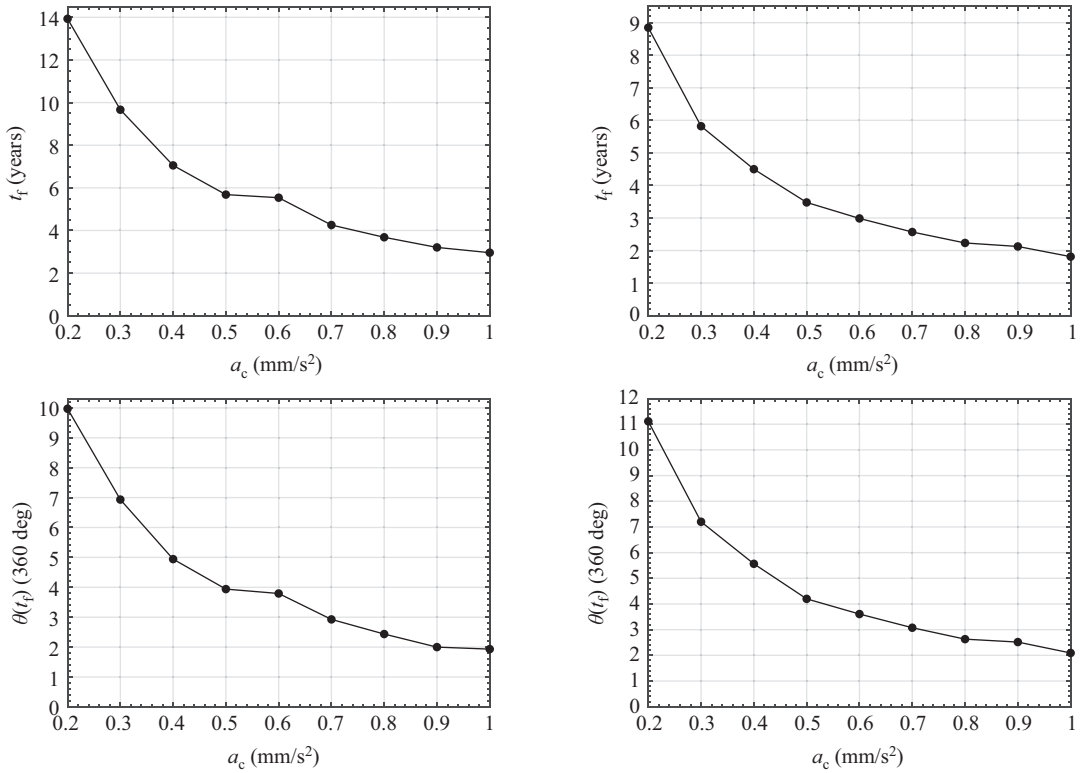

(a) Earth–Mars case (b) Earth–Venus case

Fig. 8 Variations of t_f and $\theta(t_f)$ with a_c when $\alpha_0 = 0$.

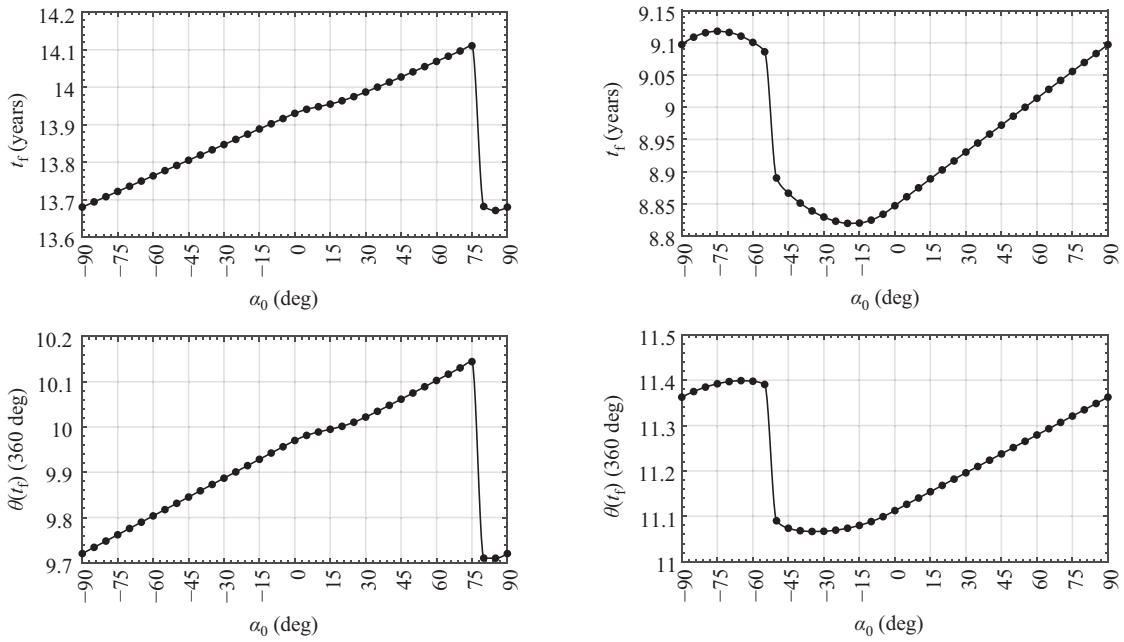

(a) Earth–Mars (b) Earth–Venus

Fig. 9 Variations of t_f and $\theta(t_f)$ with α_0 when $a_c = 0.2$ mm/s^2.

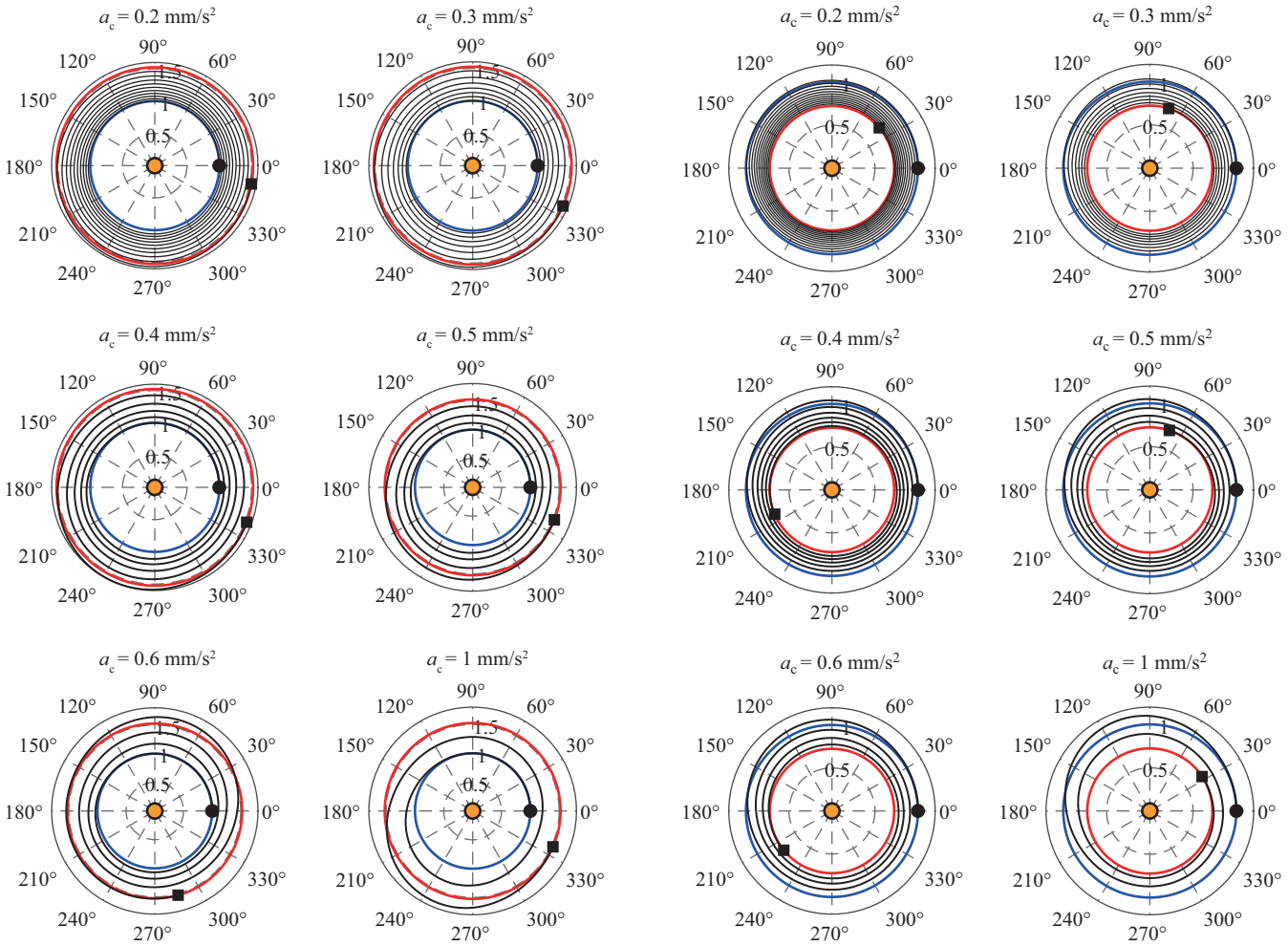

(a) Earth–Mars case (b) Earth–Venus case

Fig. 10 Optimal transfer trajectories for the two interplanetary mission scenarios.

Table 1 Comparison between the minimum flight time (t_f) of an E-sail with an inertially fixed spin axis ("fixed") and an E-sail with two control parameters ("classic"), in an Earth–Mars (EM) and an Earth–Venus (EV) circle-to-circle two-dimensional transfer

a_c (mm/s^2)	EM scenario		EV scenario	
	t_f (years) "fixed"	t_f (years) "classic"	t_f (years) "fixed"	t_f (years) "classic"
0.2	13.93	4.47	8.85	2.99
0.3	9.66	3.04	5.82	2.11
0.4	7.05	2.62	4.49	1.55
0.5	5.68	2.03	3.48	1.39
0.6	5.54	1.67	2.98	1.01
0.7	4.25	1.58	2.57	0.89
0.8	3.68	1.51	2.23	0.85
0.9	3.21	1.46	2.12	0.81
1.0	2.96	1.43	1.81	0.79

5 Conclusions

In this study, the optimal performance of a single-tether E-sail with an inertially fixed spin axis in an interplanetary framework was investigated. The trajectory optimization problem was studied using an indirect approach by obtaining a closed form of the optimal control law as a function of the spacecraft states and costates. A set of numerical simulations was used to evaluate the single-tether E-sail performance in a two-dimensional mission scenario that involved heliocentric transfer between two assigned (coplanar) circular orbits.

The numerical results indicate that the single-tether E-sail can perform optimal circle-to-circle transfer with a simplified control law that involves only the on/off state of the onboard electron emitter. Simulations also confirmed

that the near-optimal control law recently proposed in the literature can accurately describe the actual optimal transfer when a low-performance propulsion system is considered. Future work can focus on the analysis of a three-dimensional heliocentric transfer in which the variation in orbital inclination is obtained by suitably selecting both the inertial attitude of the E-sail and the switching strategy of the electron emitter.

Funding note

Open access funding provided by Università di Pisa within the CRUI-CARE Agreement.

Declaration of competing interest

The authors have no competing interests to declare that are relevant to the content of this article. The author Alessandro A. Quarta is the Associate Editor of this journal.

References

[1] Zhao, C., Huo, M. Y., Qi, J., Cao, S. L., Zhu, D. F., Sun, L. J., Sun, H. L., Qi, N. M. Coupled attitude-vibration analysis of an E-sail using absolute nodal coordinate formulation. *Astrodynamics*, **2020**, 4(3): 249–263.

[2] Huo, M. Y., Jin, R. H., Qi, J., Peng, N., Yang, L., Wang, T. C., Qi, N. M., Zhu, D. F. Rapid optimization of continuous trajectory for multi-target exploration propelled by electric sails. *Aerospace Science and Technology*, **2022**, 129: 107678.

[3] Janhunen, P. Electric sail for spacecraft propulsion. *Journal of Propulsion and Power*, **2004**, 20(4): 763–764.

[4] Janhunen, P., Sandroos, A. Simulation study of solar wind push on a charged wire: Basis of solar wind electric sail propulsion. *Annales Geophysicae*, **2007**, 25(3): 755–767.

[5] Janhunen, P., Toivanen, P. K., Polkko, J., Merikallio, S., Salminen, P., Haeggström, E., Seppänen, H., Kurppa, R., Ukkonen, J., Kiprich, S., *et al.* Electric solar wind sail: Toward test missions. *Review of Scientific Instruments*, **2010**, 81(11): 111301.

[6] Janhunen, P., Quarta, A. A., Mengali, G. Electric solar wind sail mass budget model. *Geoscientific Instrumentation, Methods and Data Systems*, **2013**, 2(1): 85–95.

[7] Fulton, J., Schaub, H. Dynamics and control of the flexible electrostatic sail deployment. In: Proceedings of the AAS/AIAA 26th Spaceflight Mechanics Meeting, **2016**: AAS 16-499.

[8] Li, G. Q., Zhu, Z. H., Du, C. G. Stability and control of radial deployment of electric solar wind sail. *Nonlinear Dynamics*, **2021**, 103(1): 481–501.

[9] Sakamoto, H., Mughal, M. R., Slavinskis, A., Praks, J., Toivanen, P., Janhunen, P., Palmroth, M., Kilpua, E., Vainio, R. Verification of tether deployment system aboard CubeSat through dynamics simulations and tests. In: Proceedings of the IEEE Aerospace Conference, **2021**: 1–7.

[10] Bassetto, M., Niccolai, L., Quarta, A. A., Mengali, G. A comprehensive review of Electric Solar Wind Sail concept and its applications. *Progress in Aerospace Sciences*, **2022**, 128: 100768.

[11] Lätt, S., Slavinskis, A., Ilbis, E., Kvell, U., Voormansik, K., Kulu, E., Pajusalu, M., Kuuste, H., Sünter, I., Eenmäe, T., *et al.* ESTCube-1 nanosatellite for electric solar wind sail in-orbit technology demonstration. *Proceedings of the Estonian Academy of Sciences*, **2014**, 63(2S): 200–209.

[12] Slavinskis, A., Pajusalu, M., Kuuste, H., Ilbis, E., Eenmae, T., Sunter, I., Laizans, K., Ehrpais, H., Liias, P., Kulu, E., *et al.* ESTCube-1 in-orbit experience and lessons learned. *IEEE Aerospace and Electronic Systems Magazine*, **2015**, 30(8): 12–22.

[13] Dalbins, J., Allaje, K., Ehrpais, H., Iakubivskyi, I., Ilbis, E., Janhunen, P., Kivastik, J., Merisalu, M., Noorma, M., Pajusalu, M., *et al.* Interplanetary student nanospacecraft: Development of the LEO demonstrator ESTCube-2. *Aerospace*, **2023**, 10(6): 503.

[14] Iakubivskyi, I., Ehrpais, H., Dalbins, J., Oro, E., Kulu, E., Kütt, J., Janhunen, P., Slavinskis, A., Ilbis, E., Ploom, I., *et al.* ESTCube-2 mission analysis: Plasma brake experiment for deorbiting. In: Proceedings of the 67th International Astronautical Congress, **2016**: IAC-16,E2,4,4,x33190.

[15] Ofodile, I., Kutt, J., Kivastik, J., Kaspar Nigol, M., Parelo, A., Ilbis, E., Ehrpais, H., Slavinskis, A. ESTCube-2 attitude determination and control: Step towards interplanetary CubeSats. In: Proceedings of the IEEE Aerospace Conference, **2019**: 1–12.

[16] Dalbins, J., Allaje, K., Iakubivskyi, I., Kivastik, J., Komarovskis, R. O., Plans, M., Sunter, I., Teras, H., Ehrpais, H., Ilbis, E., *et al.* ESTCube-2: The experience of developing a highly integrated CubeSat platform. In: Proceedings of the IEEE Aerospace Conference, **2022**: 1–16.

[17] Palos, M., Janhunen, P., Toivanen, P., Tajmar, M., Iakubivskyi, I., Micciani, A., Orsini, N., Kütt, J., Rohtsalu, A., Dalbins, J., *et al.* Electric sail mission expeditor, ESME: Software architecture and initial ESTCube lunar cubesat E-sail experiment design.

Aerospace, **2023**, 10(8): 694.

[18] Huo, M. Y., Mengali, G., Quarta, A. A. Electric sail thrust model from a geometrical perspective. *Journal of Guidance, Control, and Dynamics*, **2018**, 41(3): 735–741.

[19] Bassetto, M., Quarta, A. A., Mengali, G. Thrust model and guidance scheme for single-tether E-sail with constant attitude. *Aerospace Science and Technology*, **2023**, 142: 108618

[20] Quarta, A. A., Mengali, G. Minimum-time trajectories of electric sail with advanced thrust model. *Aerospace Science and Technology*, **2016**, 55: 419–430.

[21] Mengali, G., Quarta, A. A., Janhunen, P. Electric sail performance analysis. *Journal of Spacecraft and Rockets*, **2008**, 45(1): 122–129.

[22] Toivanen, P. K., Janhunen, P. Spin plane control and thrust vectoring of electric solar wind sail. *Journal of Propulsion and Power*, **2012**, 29(1): 178–185.

[23] Bassetto, M., Mengali, G., Quarta, A. A. E-sail attitude control with tether voltage modulation. *Acta Astronautica*, **2020**, 166: 350–357.

[24] Bryson, A. E., Ho, Y. C. *Applied Optimal Control*. New York, USA: Hemisphere Publishing Corporation, **1975**: 71–89.

[25] Stengel, R. F. *Optimal Control and Estimation*. New York, USA: Dover Publications, Inc., **1994**: 222–254.

[26] Ross, I. M. *A Primer on Pontryagin's Principle in Optimal Control*. San Francisco, USA: Collegiate Publishers, **2015**: 127–129.

[27] Morante, D., Sanjurjo Rivo, M., Soler, M. A survey on low-thrust trajectory optimization approaches. *Aerospace*, **2021**, 8(3): 88.

[28] Von Stryk, O., Bulirsch, R. Direct and indirect methods for trajectory optimization. *Annals of Operations Research*, **1992**, 37(1–4): 357–373.

[29] Bassetto, M., Quarta, A. A., Mengali, G. Locally-optimal electric sail transfer. *Proceedings of the Institution of Mechanical Engineers, Part G: Journal of Aerospace Engineering*, **2019**, 233(1): 166–179.

[30] Lawden, D. F. *Optimal Trajectories for Space Navigation*. London: Butterworths & Co., **1963**: 54–60.

Alessandro A. Quarta received his Ph.D. degree in aerospace engineering from the University of Pisa in 2005 and he currently is a professor of flight mechanics at the Department of Civil and Industrial Engineering of the University of Pisa. His main research areas include spaceflight simulation, spacecraft mission analysis and design, low-thrust trajectory optimization, and solar sail and E-sail dynamics and control. E-mail: a.quarta@ing.unipi.it

Marco Bassetto received his Ph.D. degree in industrial engineering at the Department of Civil and Industrial Engineering of the University of Pisa. After receiving his Ph.D. degree, at the same department he was first the holder of a scholarship entitled "Dynamic analysis and control of an E-sail" and then held the position of research assistant in spaceflight mechanics. From January 2023 he holds the position of assistant professor of space systems at the Department of Civil and Industrial Engineering of the University of Pisa. His research activity focuses on trajectory design and attitude control of spacecraft propelled with low-thrust propulsion systems, such as solar sails and electric solar wind sails. E-mail: marco.bassetto@unipi.it

Giovanni Mengali received his Doctor Engineer degree in aeronautical engineering in 1989 from the University of Pisa. Since 1990, he has been with the Department of Aerospace Engineering (now Department of Civil and Industrial Engineering) of the University of Pisa, first as a Ph.D. student, then as an assistant and an associate professor. Currently, he is a professor of spaceflight mechanics. His main research areas include spacecraft mission analysis, trajectory optimization, solar sails, electric sails, and aircraft flight dynamics and control. E-mail: g.mengali@ing.unipi.it